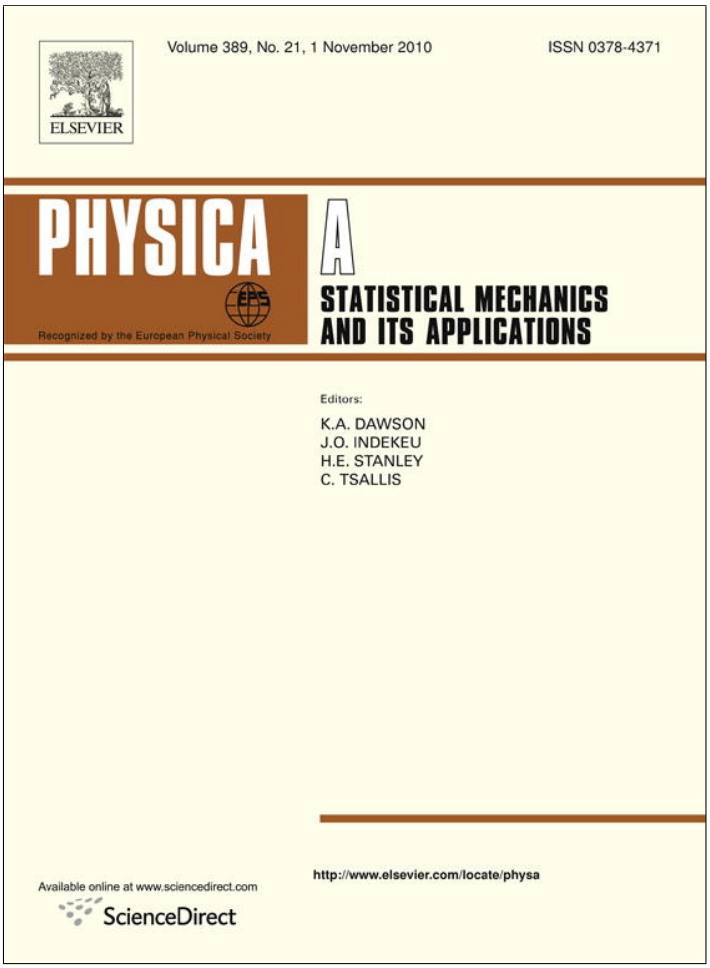

Physica A 389 (2010) 4604–4612

Contents lists available at ScienceDirect

Physica A

journal homepage: www.elsevier.com/locate/physa

Info-quantifiers' map-characterization revisited

Osvaldo A. Rosso [a,b,e,*], Luciana De Micco [c,e], A. Plastino [d,e], Hilda A. Larrondo [c,e]

[a] Departamento de Física, Instituto de Ciências Exatas, Universidade Federal de Minas Gerais, Av. Antônio Carlos, 6627 - Campus Pampulha, 31270-901 Belo Horizonte - MG, Brazil

[b] Chaos & Biology Group, Instituto de Cálculo, Facultad de Ciencias Exactas y Naturales, Universidad de Buenos Aires, Pabellón II, Ciudad Universitaria, 1428 Ciudad de Buenos Aires, Argentina

[c] Facultad de Ingeniería, Universidad Nacional de Mar del Plata, Av. J.B. Justo 4302, 7600 Mar del Plata, Argentina

[d] Instituto de Física, Facultad de Ciencias Exactas, Universidad Nacional de La Plata (UNLP), C.C. 727, 1900 La Plata, Argentina

[e] CONICET, Argentina

ARTICLE INFO

Article history:
Received 9 April 2010
Received in revised form 8 June 2010
Available online 17 July 2010

Keywords:
Information Theory
Shannon Entropy
Fisher Information Measure
Time series
Probability distribution functions
Nonlinear dynamical systems
Logistic map

ABSTRACT

We highlight the potentiality of a special Information Theory (IT) approach in order to unravel the intricacies of nonlinear dynamics, the methodology being illustrated with reference to the logistic map. A rather surprising *dynamic feature* → *plane-topography* map becomes available.

1. Introduction

A great ideal of interest exists in the behavior of dynamical systems that are highly sensitive to initial conditions, a sensitivity popularly referred to as the butterfly effect. Small differences in initial conditions (such as those due to rounding errors in numerical computation) yield widely diverging outcomes for chaotic systems, rendering long-term prediction impossible in general [1]. This happens even though these systems are deterministic and their "future" is fully determined by their initial conditions, with no random elements involved, so that the deterministic nature of these systems does not make them predictable. Explanation of such behavior may be sought in various ways, an important one being the through analysis of nonlinear models, that usually yields a wealth of interesting information.

Information theory, in turn, is a powerful weapon in the theoretical physicist's arsenal [2] that has been put to good use in the analysis just referred to, with an exuberant literature dealing with such matters (see references given below in the text). The present effort tries to add, hard as it sounds, some new ingredients to this kind of approach, and we expect to convince the readers in the forthcoming sections that this is not an empty claim.

* Corresponding author at: Chaos & Biology Group, Instituto de Cálculo, Facultad de Ciencias Exactas y Naturales, Universidad de Buenos Aires, Pabellón II, Ciudad Universitaria, 1428 Ciudad de Buenos Aires, Argentina. Tel.: +55 31 3409 6633.

E-mail addresses: oarosso@fibertel.com.ar, Osvaldo.A.Rosso@newcastle.edu.au, oarosso@gmail.com (O.A. Rosso), lucianadm55@gmail.com (L. De Micco), plastino@fisica.unlp.edu.ar (A. Plastino), larrondo@fi.mdp.edu.ar (H.A. Larrondo).

0378-4371/$ – see front matter © 2010 Elsevier B.V. All rights reserved.
doi:10.1016/j.physa.2010.06.055

2. Shannon entropy & Fisher Information Measure

Given a continuous probability distribution function (PDF) $f(x)$, its *Shannon entropy* S is [3]

$$S[f] = -\int f \ln(f) \mathrm{d}x, \tag{1}$$

a measure of "global character" that it is not too sensitive to strong changes in the distribution taking place on a small-sized region.

Such is not the case with *Fisher's information measure (FIM)* F [2,4], which constitutes a measure of the gradient content of the distribution f, thus being quite sensitive even to tiny localized perturbations. It reads [2]

$$F[f] = \int \frac{|\vec{\nabla} f|^2}{f} \mathrm{d}x. \tag{2}$$

FIM can be variously interpreted as a measure of the ability to estimate a parameter, as the amount of information that can be extracted from a set of measurements, and also as a measure of the state of disorder of a system or phenomenon [2,5]. Its most important property is the so-called Cramer–Rao bound, that we recapitulate in one-dimension, for simplicity's sake. The classical Fisher information associated with translations of a one-dimensional observable x with corresponding probability density $f(x)$ is [6]

$$I_x = \int \mathrm{d}x f(x) \left(\frac{\partial \ln f(x)}{\partial x} \right)^2, \tag{3}$$

which obeys the above referred to Cramer–Rao inequality

$$(\Delta x)^2 \geq I_x^{-1} \tag{4}$$

involving the variance of the stochastic variable x [6]

$$(\Delta x)^2 = \langle x^2 \rangle - \langle x \rangle^2 = \int \mathrm{d}x f(x) x^2 - \left(\int \mathrm{d}x f(x) x \right)^2. \tag{5}$$

We insist in remarking that the gradient operator significantly influences the contribution of minute local f-variations to FIM's value, so that the quantifier is called a "local" one. Note that Shannon's entropy decreases with skewed distribution, while Fisher's information increases in such a case. Local sensitivity is useful in scenarios whose description necessitates appeal to a notion of "order" (see below).

Let now $P = \{p_i;\ i = 1, \ldots, N\}$ be a discrete probability distribution set, with N the number of possible states of the system under study. The concomitant problem of loss of information due to the discretization has been thoroughly studied (see, for instance, [7–9] and references therein) and, in particular, it entails the loss of FIM's shift-invariance, which is of no importance for our present purposes. In the discrete case, Shannon's quantifier is evaluated via

$$S[P] = -\sum_{i=1}^{N} p_i \ln(p_i), \tag{6}$$

and we define a "normalized" Shannon entropy as $H[P] = S[P]/S_{\max}$, where the denominator obtains for a uniform probability distribution.

For the FIM-computation measure, we follow the proposal of Ferri and coworkers [10] (among others)

$$F[P] = \frac{1}{4} \sum_{i=1}^{N-1} 2 \frac{(p_{i+1} - p_i)^2}{(p_{i+1} + p_i)}. \tag{7}$$

If our system is in a very ordered state and thus is represented by a very narrow PDF, we have a Shannon entropy $S \sim 0$ and a Fisher's information measure $F \sim F_{\max}$. On the other hand, when the system under study lies in a very disordered state one gets an almost flat PDF and $S \sim S_{\max}$ while $F \sim 0$. Of course, $S_{\max}$ and $F_{\max}$ are, respectively, the maximum values for the Shannon entropy and Fisher information measure. One can state that the general behavior of the Fisher information measure is opposite to that of the Shannon entropy [11].

3. Temporal information and methodologies for getting the pertinent PDFs

Information measures are functionals of a probability distribution function (PDF). In evaluating them, one has to properly determine this underlying PDF P (here associated with a given dynamical system or time series). This is an often neglected issue that indeed deserves detailed consideration. Why? Because P and the sample-space Ω are inextricably linked. Many schemes have been proposed for an adequate selection of pair (Ω, P). We can mention, among others: (a) procedures based

on amplitude statistics [12], (b) binary symbolic dynamics [13], (c) Fourier analysis [14] and, (d) wavelet transform [15]. Their applicability depends on particular characteristics of the pertinent data such as stationarity, length of the time series, variation of the parameters, level of noise contamination, etc. In all these cases, the global aspects of the dynamics can be somehow captured, but the different approaches are not equivalent in their ability to discern all the relevant physical details. One must also acknowledge the fact that the above techniques are introduced in a *rather ad hoc fashion and are not directly derived from the dynamical properties themselves of the system under study*, as can be conveniently achieved, for instance, by recourse to the Bandt–Pompe methodology [16].

Bandt and Pompe introduced a successful approach for the evaluation of the PDF associated with scalar time series data using a symbolization technique [16,17]. The symbolic data are created by ranking the values of the series and defined (this the essential detail) by reordering the embedded data in ascending order, which is in turn reconstructed with an embedding dimension D (see definition and methodological details below). *"Causal" information* is, consequently, properly incorporated into the "building-up" process that yields (Ω, P) [16,17]. In this way it is possible to quantify the diversity of the ordering symbols (patterns) derived from a scalar time series, evaluating the so called permutation entropy (the Shannon entropy special version corresponding to the Bandt and Pompe PDF). The Bandt and Pompe technique is computationally fast and does not require the reconstruction of an attractor in phase space. It is the only procedure, among those most currently used, that takes into account the temporal structure of the time series generated by the physical process under study. An additional advantage of using this approach is that it is based on quite weak stationarity assumptions, a property that allows one to uncover important details concerning the ordinal structure of the time series [12,18–27], and can also reveal information about temporal correlations [28,29].

3.1. PDF based on histograms

In order to extract a PDF via amplitude statistics, divide first the interval $[a, b]$ (with a and b the minimum and maximum values in the time series) into a finite number N_{nbin} of nonoverlapping subintervals $A_i : [a, b] = \bigcup_{i=1}^{N_{\text{nbin}}} A_i$ with $A_i \bigcap A_j = \emptyset \, \forall i \neq j$. One then employs the usual histogram method, based on counting the relative frequencies of the time series' values within each subinterval. It should be clear that the resulting PDF lacks any information regarding temporal evolution. The only pieces of information we have here are the x_t-values that allow one to assign inclusion within a given bin, ignoring just where they are located (this is, the subindex i). Note that in Eqs. (6) and (7) $N = N_{\text{bin}}$ and that the division procedure of the interval $[a, b]$ provides the natural order sequence for the evaluation of the PDF gradient involved in Fisher's information measure. Let us also point out that it is relevant to consider a judiciously chosen optimal value for N_{bin} (see i.e. De Micco et al. [12]). The information measures obtained via histogram PDFs are called in this paper $H^{(\text{Hist})}$ and $F^{(\text{Hist})}$, respectively.

3.2. PDF based on Bandt and Pompe methodology

To use the Bandt and Pompe [16] methodology for evaluating probability distribution P associated with the time series (for a given dynamical system) under study one starts by considering partitions of the pertinent D-dimensional space that will hopefully "reveal" relevant details of the ordinal structure of this time series $\{x_t : t = 1, \ldots, M\}$ with embedding dimension $D > 1$. We are interested in "ordinal patterns" of order D [16,19] generated by

$$(s) \mapsto \left(x_{s-(D-1)}, x_{s-(D-2)}, \ldots, x_{s-1}, x_s\right), \tag{8}$$

which assign to each time s the D-dimensional vector of values at times $s, s-1, \ldots, s-(D-1)$. Clearly, the greater the D-value, the more information on the past is incorporated into our vectors. By the "ordinal pattern" related to the time (s), we mean the permutation $\pi = (r_0, r_1, \ldots, r_{D-1})$ of $(0, 1, \ldots, D-1)$ defined by

$$x_{s-r_{D-1}} \leq x_{s-r_{D-2}} \leq \cdots \leq x_{s-r_1} \leq x_{s-r_0}. \tag{9}$$

In order to get a unique result, we set $r_i < r_{i-1}$ if $x_{s-r_i} = x_{s-r_{i-1}}$. Thus, for all the $D!$ possible permutations π of order D, the probability distribution $P = \{p(\pi)\}$ is defined by

$$p(\pi) = \frac{\sharp\{s | s \leq M - D + 1; (s), \ \texttt{has type}\ \pi\}}{M - D + 1}. \tag{10}$$

In this expression, the symbol $\sharp$ stands for "number". For the computation of the Bandt and Pompe PDF, we follow the very fast algorithm described by Keller and Sinn in Ref. [19], in which the different ordinal patterns are generated in lexicographic ordering and this is the order sequence used in the evaluation of the PDF gradient involved in the Fisher information measure. The two information measures obtained via the ensuing Bandt and Pompe PDF are called in this paper $H^{(\text{BP})}$ and $F^{(\text{BP})}$.

The Bandt–Pompes methodology is not restricted to time series representatives of low dimensional dynamical systems but can be applied to any type of time series (regular, chaotic, noisy, or reality based), with a very weak stationary assumption (for $k = D$, the probability for $x_t < x_{t+k}$ should not depend on t [16]). One also assumes that enough data are available for a correct attractor reconstruction. Of course, the embedding dimension D plays an important role in the evaluation of the appropriate probability distribution because D determines the number of accessible states $D!$. Also, it conditions the minimum acceptable length $M \gg D!$ of the time series that one needs in order to work with a reliable statistics.

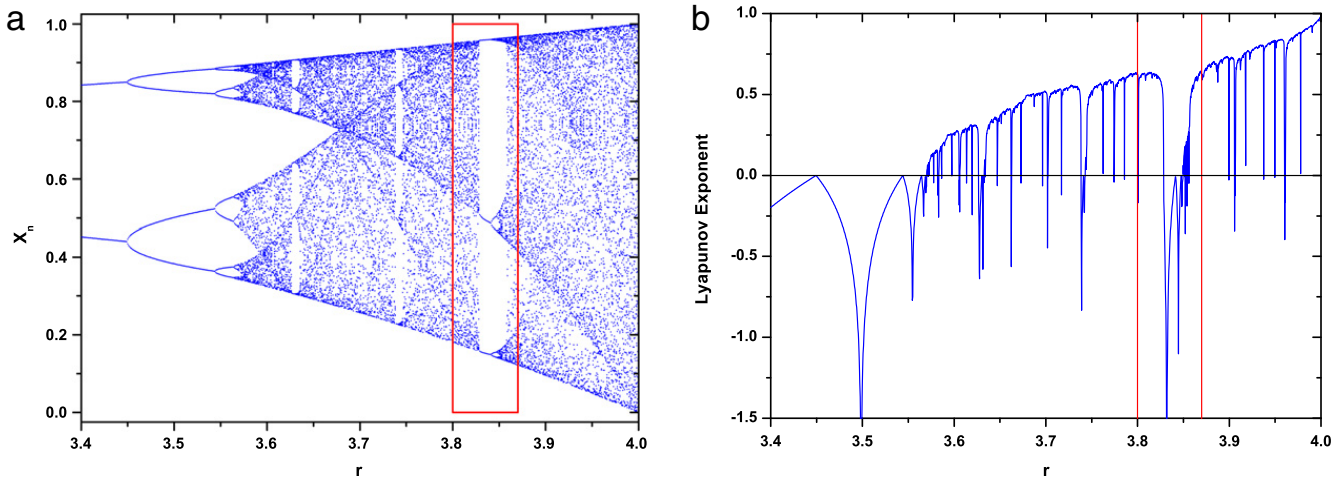

Fig. 1. (a) Bifurcation diagram ($\Delta r = 0.001$) and (b) Lyapunov exponent Λ ($\Delta r = 0.0003$), for the logistic map as a function of the parameter r.

4. Application to the logistic map

The logistic map constitutes a paradigmatic example, often employed as a testing ground in order to illustrate new concepts in the treatment of dynamical systems. Thus, we will use it in order to exemplify the behavior of two quantifiers based on Information Theory, namely, the normalized Shannon entropy H and Fisher's information measure F, both evaluated with PDFs based on either histograms or Bandt–Pompe's procedure.

It is well known that the logistic map is a polynomial mapping of degree 2, $F : x_n \to x_{n+1}$ [30,31], described by the ecologically motivated, dissipative system described by the first-order difference equation

$$x_{n+1} = r \cdot x_n \cdot (1 - x_n) \tag{11}$$

with $0 \leq x_n \leq 1$ and $0 < r \leq 4$. Fig. 1(a) depicts the popular bifurcation diagram for the logistic map for $3.4 \leq r \leq 4.0$ ($\Delta r = 0.001$), while, in Fig. 1(b), the corresponding Lyapunov exponent Λ ($\Delta r = 0.0003$) is displayed.

Let us briefly review, with reference to Fig. 1, some exceedingly well-known results for this map that we need in order to put into an appropriate perspective the properties of our quantifiers. For values of the control parameter $1 < r < 3$, there exists only a single steady-state solution. Increasing the control parameter past $r = 3$ forces the system to undergo a period-doubling bifurcation. Cycles of period 8, 16, 32, ..., occur and, if r_n denotes the value of r where a 2^n cycle first appears, the r_n converge to a limiting value $r_\infty \cong 3.5699456$ [30,31]. As r grows still more, a quite rich, and well-known structure arises. In order to be in a position to better appreciate at once the long-term behavior for all values of r lying between 3.4 and 4.0, we plot the pertinent bifurcation diagram in Fig. 1(a). We immediately note there the cascade of further period doubling that occurs as r increases, until, at r_∞, the maps become chaotic and the attractors change from comprising a finite set of points to becoming an infinite set. For $r > r_\infty$ the orbit diagram reveals an "strange" mixture of order and chaos. The large window beginning near $r \cong 3.82842$ contains a stable period-3 cycle.

The behavior of the Lyapunov exponent Λ as a function of the parameter r is displayed in Fig. 1(b). From this figure, we see that Λ and, as a result, the associated degree of chaoticity grows globally with r since there are many periodic windows where Λ drops to negative values, reaching a maximum at $r = 4$. The non-zero Lyapunov characteristic exponent Λ remains negative for $r < r_\infty$. We notice that Λ approaches zero at the period-doubling bifurcation. The onset of chaos is apparent near $r \cong 3.5699$, where Λ first becomes positive. As stated above, for $r > r_\infty$, the Lyapunov exponent increases globally, except for the dips one sees in the windows of periodic behavior. Notice the particularly large dip due to the period-3 window near $r \cong 3.82842$.

Following the work of Ferri et al. [10] and in order to facilitate the comparison with their results, we scrutinize the dynamics of the logistic map around this period-3 window. In particular, we analyze the logistic parameter range $3.8 \leq r \leq 3.87$ demarcated with the rectangle in Fig. 1(a) and with vertical lines in Fig. 1(b). The bifurcation diagram ($\Delta r = 0.0005$) and the corresponding Lyapunov exponent ($\Delta r = 1 \times 10^{-5}$) are displayed for this parameter range in Fig. 2. With this rather fine resolution one detects the presence of additional periodic windows, dips in which the Lyapunov exponent is $\Lambda < 0$ in Fig. 2(b).

The period-3 attractor arises through a saddle-node bifurcation at $r_1 \cong 3.82842$ (tangent bifurcation) till $r_2 \cong 3.8415$ (flip bifurcation). The chaotic dynamics that exists before reaching r_1 is called "Chaos 1". As r grows beyond r_2, the period-3 solutions experience a new sequence of period-doubling bifurcations that ends in a totally chaotic dynamics at $r_3 \cong 3.84943$. The chaotic attractor consists of three narrow disjoint segments and is referred to as "Chaos 2". At $r_4 \cong 3.85681$ (interior crisis) this chaotic attractor is again replaced by another one designed as "Chaos 3" which lives within a wider segment that includes the three parts of the previous attractor. For $r_2 < r < r_4$, the period-3 window expanded in Fig. 2(a) shows three miniature bifurcation diagrams that are similar to the large one in Fig. 1(a). Note that in similar fashion as with the boundary crisis at $r = 4$, these smaller regions suddenly expand at r_4 to fill a single wider interval.

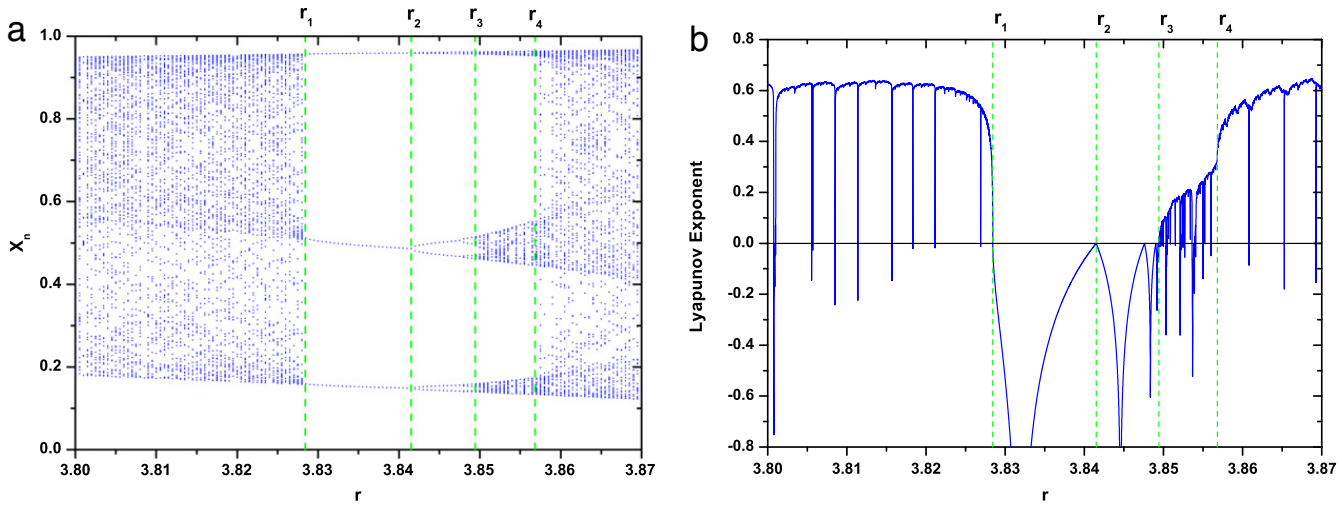

Fig. 2. (a) Bifurcation diagram ($\Delta r = 0.0005$) and (b) Lyapunov exponent Λ ($\Delta r = 1 \times 10^{-5}$), for the logistic map as a function of the parameter $3.8 \leq r \leq 3.87$.

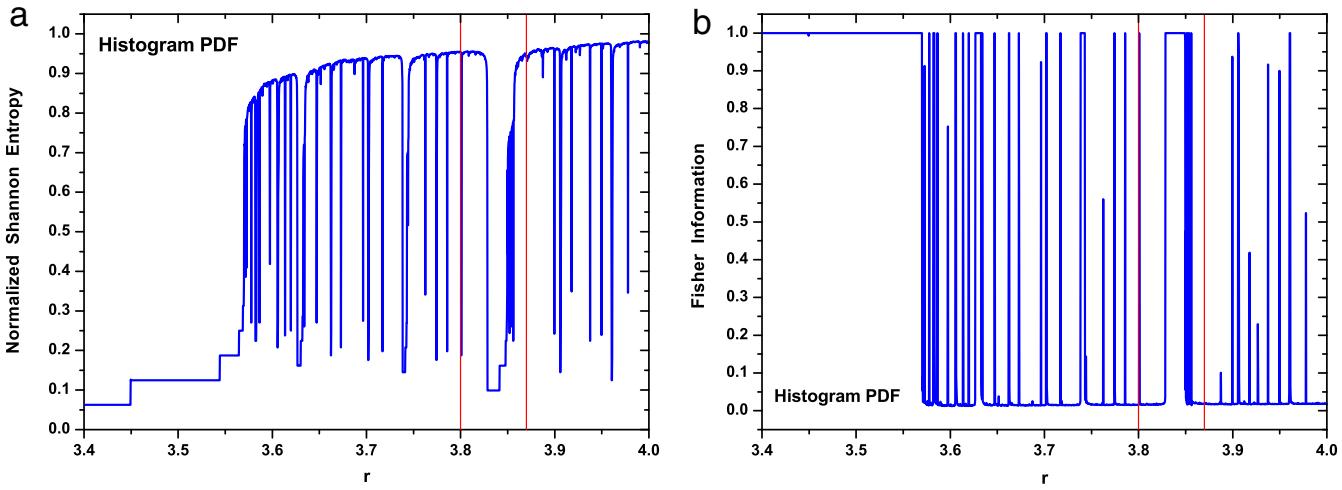

Fig. 3. (a) Normalized Shannon entropy and, (b) Fisher information measure for the logistic map as function of the parameter $3.4 \leq r \leq 4$ with step $\Delta r = 0.0003$. For the time series generation, we discard the first 10^5 iterations and after that $N = 2 \times 10^6$ data time series was generated. For the PDF based on histogram Procedure, we considered $N_{\text{bins}} = 2^{16}$ in the interval [0, 1].

The behavior of our information theory quantifiers: the normalized Shannon entropy, H and, Fisher information measure, F, as functions of the logistic parameter r are displayed in Figs. 3 and 5 for $3.4 \leq r \leq 4$; $\Delta r = 0.0003$; Figs. 4 and 6 for $3.8 \leq r \leq 3.87$; $\Delta r = 1 \times 10^{-5}$; for PDFs based on histograms and Bandt–Pompe's methodology, respectively. For the logistic map time series generation, we discarded the first 10^5 iterations and, after that, $N = 2 \times 10^6$ data were generated. For the PDF based on the histogram procedure, we considered $N_{\text{bins}} = 2^{16}$ in the interval [0, 1]. For the Bandt–Pompe based PDF, we fixed the patterns' length at $D = 6$.

For values of the parameter r for which a periodic window is associated, the corresponding PDF consist of a few $p_i \neq 0$ values. That is, in the case of the "PDF histogram" a few bins i will have nonzero probabilities. Note that for the PDF histogram, all the bins are duly considered, including those for which $p_i = 0$, instead of just eliminating them as Ferri et al. [10] do. In the case of a PDF of the Bandt and Pompe type, only few patterns of the total $D!$ will be observed. Accordingly, for periodic behavior the normalized Shannon entropy (NSE) will take low values, indicating that the system is "well ordered". Contrarywise, the FIM for this situation should be large since it is associated with derivatives of the PDF. Comparing the corresponding bifurcation diagram and Lyapunov exponent as a function of the logistic parameter (see Figs. 1 and 2) with the information theory quantifiers H and F (Figs. 3–6), it is clear that observed dips in the normalized Shannon entropy H and peaks in the Fisher information measure F correspond to periodic windows, a fact that cannot be appreciated in the bifurcation diagram. This is due to the fact that, in order to observe these extremes one needs a much finer resolution in the pertinent drawings. Both information quantifiers H and F detect period doubling. It is worth of note to focus attention on the transition delimiters between different dynamical regimes.

The NSE and FIM for the logistic parameter range $3.4 \leq r \leq 4$ are displayed in Figs. 3 and 5. For $r < r_\infty$ low entropy values are found, corresponding to periodic behavior. We observe in all instances an abrupt entropy growth around

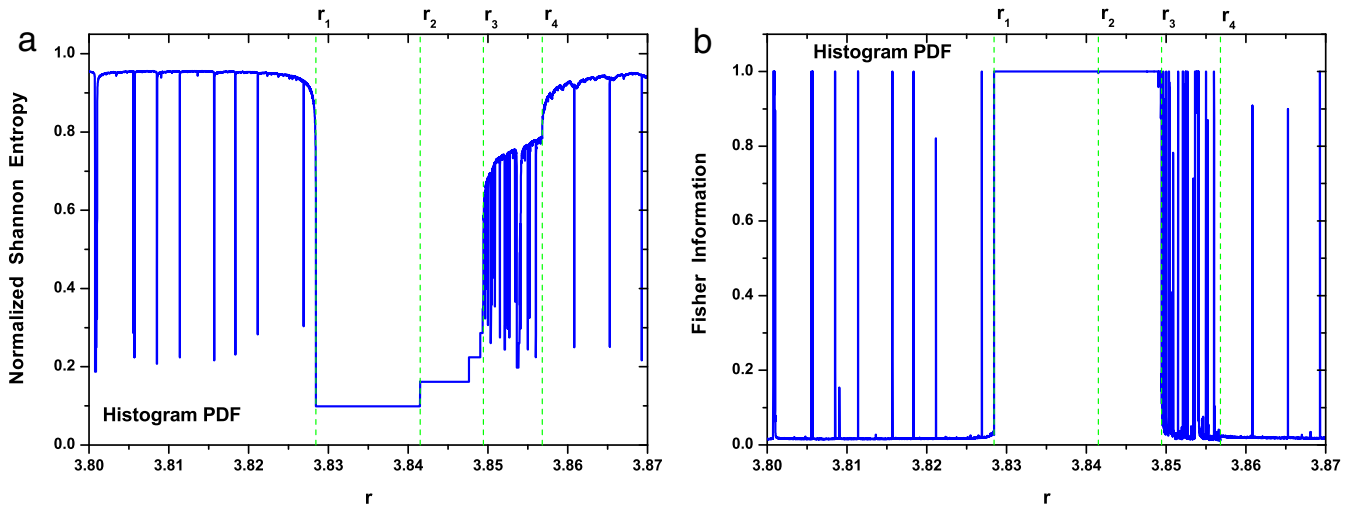

Fig. 4. (a) Normalized Shannon entropy and, (b) Fisher information measure for the logistic map as a function of the parameter $3.8 \leq r \leq 3.87$ with step $\Delta r = 1 \times 10^{-5}$. For the time series Generation, we discard the first 10^5 iterations and after that $N = 2 \times 10^6$ data time series was generated. For the PDF based on histogram procedure, we considered $N_{\text{bins}} = 2^{16}$ in the interval [0, 1].

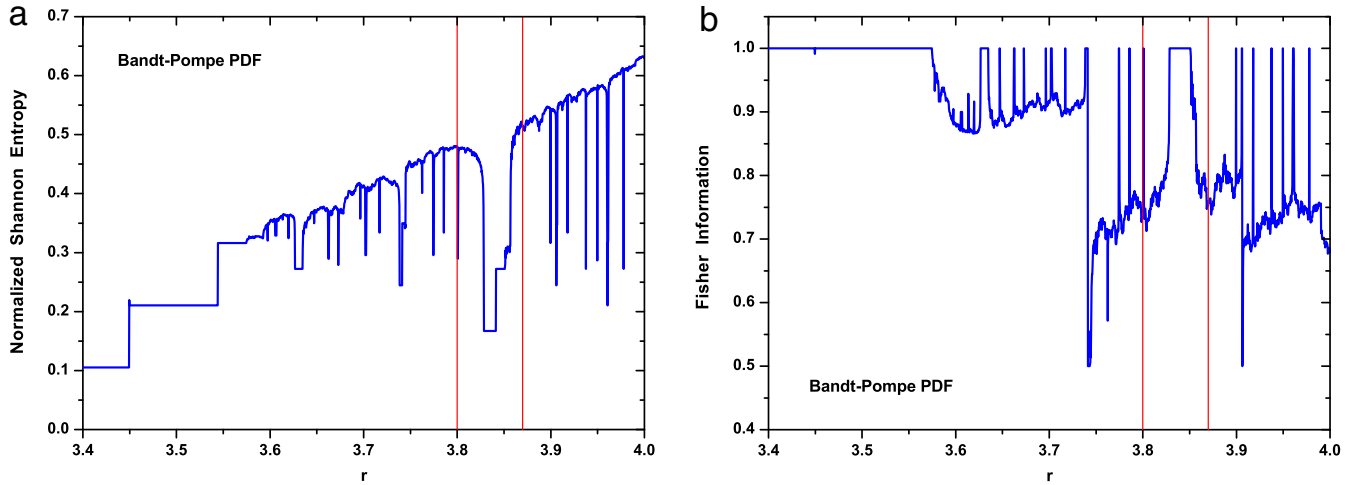

Fig. 5. (a) Normalized Shannon entropy and, (b) Fisher information measure for the logistic map as a function of the parameter $3.4 \leq r \leq 4$ with step $\Delta r = 0.0003$. For the time series generation, we discard the first 10^5 iterations and after that $N = 2 \times 10^6$ data time series was generated. For the PDF based on Bandt–Pompe Methodology, we considered $D = 6$.

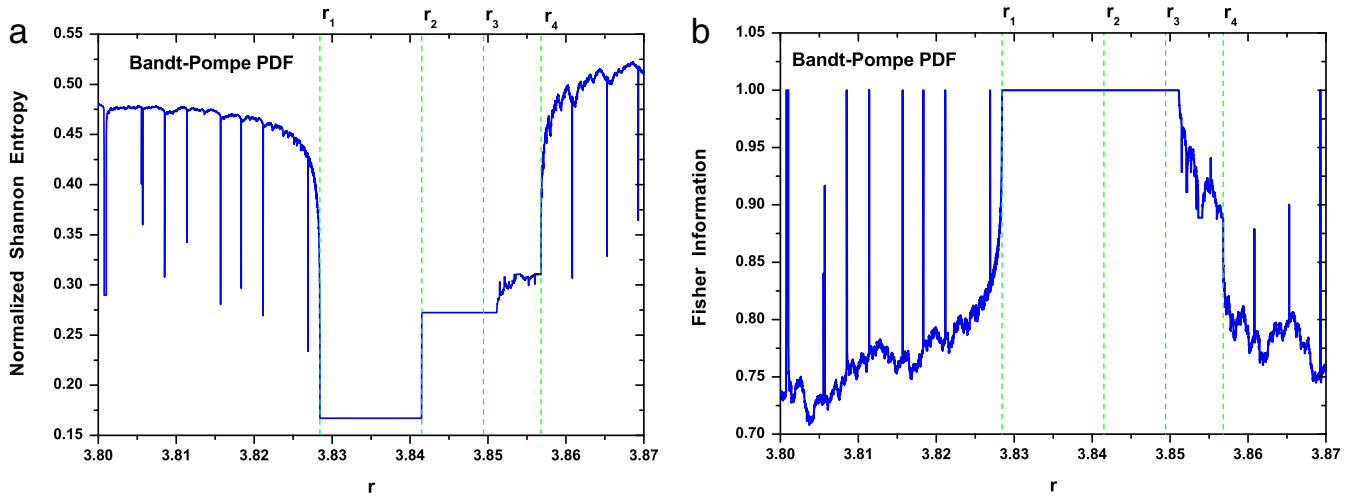

Fig. 6. (a) Normalized Shannon entropy and, (b) Fisher information measure for the logistic map as a function of the parameter $3.8 \leq r \leq 3.87$ with step $\Delta r = 1 \times 10^{-5}$. For the time series Generation, we discard the first 10^5 iterations and after that $N = 2 \times 10^6$ data time series was generated. For the PDF based on Bandt–Pompe methodology, we considered $D = 6$.

$r > r_\infty \cong 3.5699$ (see Figs. 3(a) and 5(a)). After we leave this point behind, the entropy displays an increasing trend, acquiring its maximum value at $r = 4$. The several "drops" in entropic values in the interval $r_\infty < r < 4$ correspond to the periodic windows (see the details for range $3.8 \leq r \leq 3.87$ in Figs. 3(b) and 5(b)), as can easily be confirmed by comparing with the bifurcation diagram and with the Lyapunov exponent depicted in Figs. 1 and 2. Note also that for the window $3.8 \leq r \leq 3.87$, the $H^{(\mathrm{Hist})}$ entropy exhibits similar values for the regions called "Chaos 1" and "Chaos 3". Only "Chaos 2" dynamics exhibit lower entropic values. Also notice the increasing entropy values for the period-3 zone ($r_1 < r < r_2$) and also the increasing values attained for the period 6 and period 12 ($r_2 < r < r_3$) instances. It is interesting to point out that, in the PDF-histogram instance, the entropy for $r = 4$ is almost unity ($H^{(\mathrm{Hist})} \simeq 0.977$). The reason is that the invariant measure of the logistic map is in this case given by an almost constant function [30,31]. Only the PDF Bandt and Pompe leads to the realistic value $H^{(\mathrm{BP})} \simeq 0.630$ (more about this point is elucidated below).

As previously mentioned, FIM's behavior is opposite to NSE's, as is clearly appreciated in Figs. 3(b), 4, 5 and 6(b). For $r < r_\infty$ FIM exhibits constant values $F^{(\mathrm{Hist})} = F^{(\mathrm{BP})} = 1$, with the exception of small dips at the transition, doubling-period points. For parameters values $r_\infty < r < 4$ histogramic-FIM $F^{(\mathrm{Hist})}$ displays almost null values, indicative of chaotic behaviors, alternating with sharp peaks. Comparison with the bifurcation diagram and the Lyapunov exponent (see Figs. 1 and 2) indicates that these peaks are correlated with the emergence of periodic windows. Consequently, they signal the transition between different dynamical behaviors, i.e., from chaotic to periodic ones.

It is worthy of note to scrutinize the behavior of our quantifiers, evaluated either with PDF histograms or à la PDF-Bandt and Pompe, in the vicinity of r-values, to be called r_T, at which transitions between different dynamical regimes take place. At $r \sim r_1$ one finds a transition between Chaos 1 and period 3 regimes. For small values $r \leq r_1$ typical orbits exhibit intermittencies that separate time-intervals of quasi-periodic motion. These intermittencies "explore" in sporadic fashion the remainder of the attractor. The $H^{(\mathrm{His})}$ and $F^{(\mathrm{His})}$ (see Fig. 4) evince a very sharp transition in their respective values at r_T. Contrary-wise, for $H^{(\mathrm{BP})}$ and $F^{(\mathrm{BP})}$, a smooth transition is there observed. For $r \sim r_2$ a period doubling is observed, corresponding to period 3 to period 6 change overs, highlighted by increasing values of $H^{(\mathrm{His})}$ and $H^{(\mathrm{BP})}$. FIMs values $F^{(\mathrm{His})} = F^{(\mathrm{BP})} = 1$ save for a very small decrease for r_2, where de bifurcation occurs. This behavior is not observed in the respective figures due to the scale's size. A similar situation is observed in the parameter interval $r_2 < r < r_3$, where subsequent period-duplications take place.

At the parameter range $r_3 < r < r_4$ another remarkable feature emerges, a "band splitting" phenomenon. The iterates alternates between three bands in periodic fashion. However, inside each band motion is chaotic. For $r \sim r_3$ a period-doubling accumulation event is observed and a transition to a chaotic regime comes about. Note also that inside each band several periodic windows are detected. We denote this parameter region as "Chaos 2 with periodic window". If $r > r_4$ the attractor still remains chaotic but consist now of a rather large interval that contains inside it the above mentioned small periodic windows. We speak of an interior crisis [30,31]. We designate this region as the Chaos 3-one. The values-trend of $H^{(\mathrm{His})}$ is here lower (excluding the dips corresponding to the periodic windows) for $r_3 < r < r_4$ than for $r > r_4$. Summing up, the values for $H^{(\mathrm{His})}$ are lower for the Chaos 2 zone than for the corresponding ones for Chaos 1 and Chaos 3. However, for these last two chaotic zones, their $H^{(\mathrm{His})}$-values are similar. $F^{(\mathrm{His})} \sim 0$ for Chaos 1, 2 and 3 zones, with the exception of the peaks corresponding to periodic windows.

The values of $H^{(\mathrm{BP})}$ and $F^{(\mathrm{BP})}$ display a trend that clearly distinguishes amongst the different chaotic behaviors (Chaos 1, 2 and 3 zones). Again the NSE-drops FIM-peaks for periodic windows become evident (cf. Fig. 6). This fact clearly constitutes the main advantage of using a PDF that takes into account temporal-causality in the evaluation of the quantifiers. The NSE evaluated with a PDF-Bandt and Pompe, $H^{(\mathrm{BP})}$, incorporates in a seemingly natural way "time causality", which together with the properties of the quantifier referred to as the "statistical complexity" allows in fact for the possibility of distinguishing between chaotic and stochastic dynamics [18]. Indeed, if time-causality is not properly taken into account, as is the case of PDF histograms, one has $H^{(\mathrm{Hist})} \cong 1$ for both kind of dynamics, in contradiction to what happens using the Bandt and Pompe methodology to determine the PDF, for which the situation $H^{(\mathrm{BP})} \cong 1$ is only attained in the case of stochastic (noise) dynamics [18]. In plain words, "chaos is not noise" even if they share some common characteristics. In point of fact, chaos is representative of deterministic processes, and thus time-causality constitutes an important facet that must be taken into account for a proper characterization.

One gets some important complementary insights of this situation via the Vignat–Bercher's Fisher–Shannon ($F \times H$) plane [32–36], that we will employ to characterize our different dynamic-regimes. We display in Figs. 7 and 8 this $F \times H$-plane for the two different instances of PDF-evaluation under consideration, for the r-ranges $3.4 \leq r \leq 4$ and $3.8 \leq r \leq 3.87$ (the control parameter does not explicitly appear in the graph, of course), respectively. We see that a wealth of "geographic information" regarding plane-locations for different kinds of dynamics becomes then available, a sort of *dynamic feature* → *plane-topography* map, which constitutes a rather surprising correspondence between dynamics an planar geometry.

Comparing the results obtained using PDF histograms with PDF-BP ones in Figs. 7 and 8, it becomes clear that in the last case these characteristics are more clearly evidenced, facilitating in this way planar behavior-characterization (see, in particular, Fig. 8). We can readily appreciate the fact that each distinct regime is located at different planar location.

5. Conclusions

The main idea of the present contribution has been to underline the potentiality of a special Information Theory approach in order to unravel the intricacies of nonlinear dynamics, the methodology being illustrated with reference to the logistic

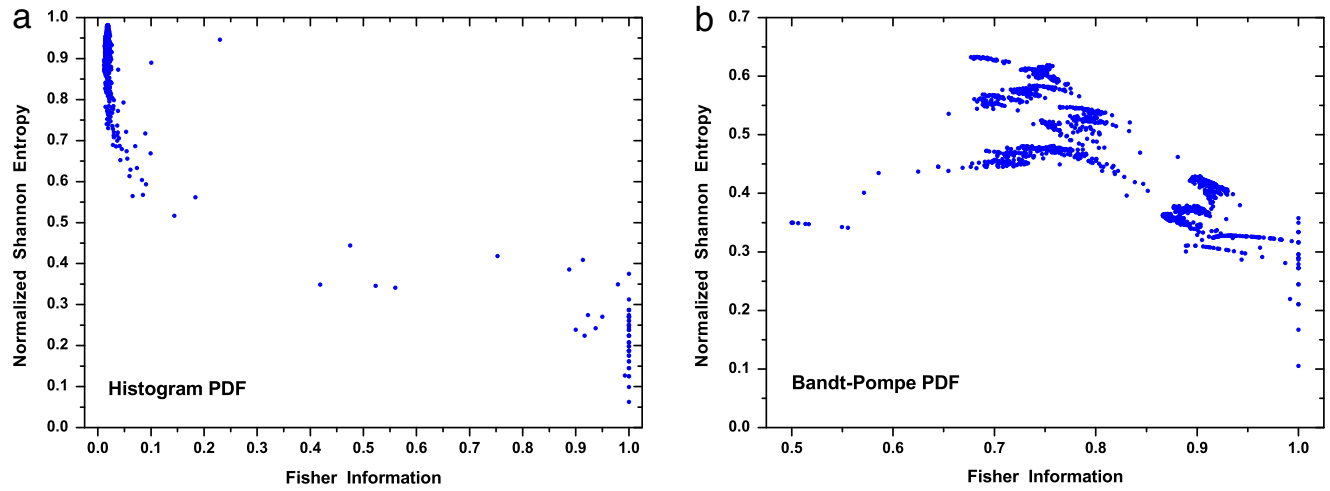

Fig. 7. Fisher–Shannon plane corresponding to (a) PDF based on histograms (b) PDF based on Bandt–Pompe procedure, for the logistic map in the parameter range $3.4 \leq r \leq 4$.

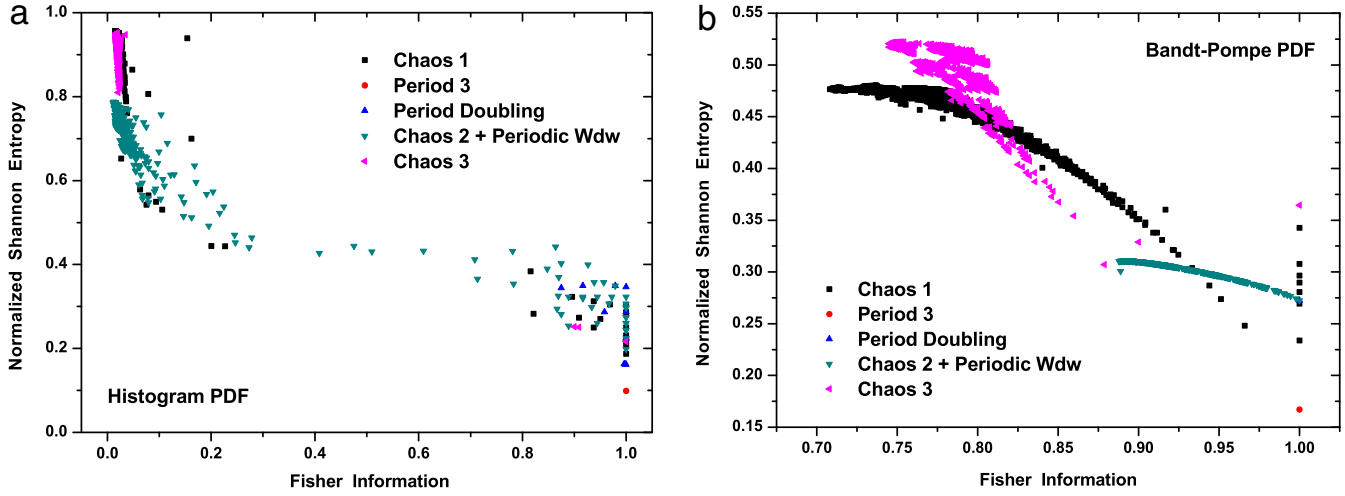

Fig. 8. Fisher–Shannon plane corresponding to (a) PDF based on histograms (b) PDF based on Bandt–Pompe procedure, for the logistic map in the parameter range $3.8 \leq r \leq 3.87$.

map. The central facets of the approach are that of (i) extracting out of the pertinent time series the most suitable probability distribution function P in order to describe the associated dynamics: This PDF is obtained by recourse to the Bandt–Pompe technique [16] and (ii) constructing with this PDF two Information Theory quantifiers, namely, a NSE and FIM. These quantifiers's results are in turn compared with those produced by the usual histogram methodology. A first conclusion is that the latter methodology is clearly inferior to the former.

More importantly, we have shown in the preceding section that the present approach is able to reveal extremely fine details of the dynamics, not easily available otherwise. Out of the two Information Theory quantifiers we have constructed the so-called Fisher–Shannon plane. Trajectories in the plane disclose novel dynamics features, even in such an well-known model as the logistic one. We conclude by suggesting that an extremely powerful treatment for uncovering delicate aspects of nonlinear physics has been advanced.

The present effort leaves open some possibilities for future research. We intend to perform further work related to the possible detection of real periodic and quasi-periodic behavior different from the one studied here, i.e., not in a window of periodicity but obtained through a Hopf bifurcation where the Lyapunov exponent touches zero and stays quasi-periodically there. We note also that Fig. 8(b) suggests that there may exist a missing dimension that would serve to separate each dynamical behavior, a tantalizing possibility.

Acknowledgements

We wish to thank Dr. Carlos Riveros for very useful discussions and comments on the current manuscript. This work was partial support from the Consejo Nacional de Investigaciones Científicas y Técnicas (CONICET), Argentina. O.A. Rosso gratefully acknowledge support from CAPES, PVE fellowship, Brazil.

References

[1] Stephen H. Kellert, In the Wake of Chaos: Unpredictable Order in Dynamical Systems, University of Chicago Press, 1993.
[2] B. Roy Frieden, Science from Fisher Information: A Unification, Cambridge University Press, Cambridge, 2004.
[3] C. Shannon, W. Weaver, The Mathematical Theory of Communication, University of Illinois Press, Champaign, IL, 1949.
[4] R.A. Fisher, On the mathematical foundations of theoretical statistics, Philos. Trans. R. Soc. Lond. Ser. A 222 (1922) 309.
[5] A.L. Mayer, C.W. Pawlowski, H. Cabezas, Fisher information and dinamic regime changes in ecological systems, Ecol. Model. 195 (2006) 72.
[6] M.J.W. Hall, Quantum properties of classical Fisher information, Phys. Rev. A 62 (2000) 012107.
[7] K. Zografos, K. Ferentinos, T. Papaioannou, Discrete approximations to the Csiszár, Renyi, and Fisher measures of information, Canad. J. Statist. 14 (1986) 355.
[8] L. Pardo, D. Morales, K. Ferentinos, K. Zografos, Discretization problems on generalized entropues and *R*-divergences, Kybernetika 30 (1994) 445.
[9] M. Madiman, O. Johnson, I. Kontoyiannis, Fisher information, compound Poisson approximation, and the Poisson channel, IEEE Int. Symp. Inform. Th., Nice (2007).
[10] G.I. Ferri, F. Pennini, A. Plastino, LMC-complexity and various chaotic regimes, Phys. Lett. A 373 (2009) 2210.
[11] F. Pennini, A. Plastino, Reciprocity relations between ordinary temperature and the Frieden–Soffer Fisher temperature, Phys. Rev. E 71 (2005) 047102.
[12] L. De Micco, C.M. Gonzalez, H.A. Larrondo, M.T. Martín, A. Plastino, O.A. Rosso, Randomizing nonlinear maps via symbolic dynamics, Physica A 387 (2008) 3373.
[13] K. Mischaikow, M. Mrozek, J. Reiss, A. Szymczak, Construction of symbolic dynamics from experimental time series, Phys. Rev. Lett. 82 (1999) 1114.
[14] G.E. Powell, I.C. Percival, A spectral entropy method for distinguishing regular and irregular motion of Hamiltonian systems, J. Phys. A: Math. Gen. 12 (1979) 2053.
[15] O.A. Rosso, M.L. Mairal, Characterization of time dynamical evolution of electroencephalographic records, Physica A 312 (2002) 469.
[16] C. Bandt, B. Pompe, Permutation entropy: a natural complexity measure for time series, Phys. Rev. Lett. 88 (2002) 174102.
[17] C. Bandt, G. Keller, B. Pompe, Entropy of the interval maps via permutations, Nonlinearity 15 (2002) 1595.
[18] O.A. Rosso, H.A. Larrondo, M.T. Martín, A. Plastino, M.A. Fuentes, Distinguishing noise from Chaos, Phys. Rev. Lett. 99 (2007) 154102.
[19] K. Keller, M. Sinn, Ordinal analysis of time series, Physica A 356 (2005) 114.
[20] A.M. Kowalski, M.T. Martín, A. Plastino, O.A. Rosso, Bandt–Pompe approach to the classical-quantum transition, Physica D 233 (2007) 21.
[21] O.A. Rosso, L. Zunino, D.G. Pérez, A. Figliola, H.A. Larrondo, M. Garavaglia, M.T. Martín, A. Plastino, Extracting features of Gaussian self-similar stochastic processes via the Bandt and Pompe approach, Phys. Rev. E 76 (2007) 061114.
[22] O.A. Rosso, R. Vicente, C. Mirasso, Encryption test of pseudo-aleatory messages embedded on chaotic laser signals: an information theory approach, Phys. Lett. A 372 (2008) 1018.
[23] L. Zunino, D.G. Pérez, M.T. Martín, M. Garavaglia, A. Plastino, O.A. Rosso, Permutation entropy of fractional Brownian motion and fractional Gaussian noise, Phys. Lett. A 372 (2008) 4768.
[24] L. Zunino, D.G. Pérez, A. Kowalski, M.T. Martín, M. Garavaglia, A. Plastino, O.A. Rosso, Fractional Brownian motion, fractional Gaussian noise, and Tsallis permutation entropy, Physica A 387 (2008) 6067.
[25] L. De Micco, H. Larrondo, A. Plastino, O.A. Rosso, Quantifiers for stochasticity of chaotic pseudo random number generators, Philos. Trans. R. Soc. Lond. Ser. A 367 (2009) 3281.
[26] L. Zunino, M. Zanin, B.M. Tabak, D. Pérez, O.A. Rosso, Forbidden patterns, permutation entropy and stock market inefficiency, Physica A 388 (2009) 2854.
[27] L. Zunino, M. Zanin, B.M. Tabak, D. Pérez, O.A. Rosso, Complexity-entropy causality plane: a useful approach to quantify the stock market inefficiency, Physica A 389 (2010) 1891.
[28] O.A. Rosso, C. Masoller, Detecting and quantifying stochastic and coherence resonances via information theory complexity measurements, Phys. Rev. E 79 (2009) 040106(R).
[29] O.A. Rosso, C. Masoller, Detecting and quantifying temporal correlations in stochastic resonance via information theory measures, Eur. Phys. J. B 69 (2009) 37.
[30] J.C. Sprott, Chaos and Time Series Analysis, Oxford University Press, Oxford, 2004.
[31] E. Ott, T. Sauer, J.A. Yorke, Coping With Chaos, Wiley, New York, 1994.
[32] C. Vignat, J.F. Bercher, Analysis of signals in the Fisher–Shannon information plane, Phys. Lett. A 312 (2003) 27.
[33] E. Romera, J.D. Dehesa, The Fisher–Shannon information plane an electron correlation tool, J. Chem. Phys. 120 (2004) 8906.
[34] K.D. Sen, J. Antolin, J.C. Angulo, Fisher–Shannon analysis of ionization processes and isoelectron series, Phys. Rev. A 76 (2007) 032502.
[35] J.B. Szabó, K.D. Sen, A. Nagy, Fisher–Shannon information plane for atoms, Phys. Lett. A 372 (2007) 2428.
[36] J.C. Angulo, J. Antonin, K.D. Sen, Fisher–Shannon plane and statistical complexity for atoms, Phys. Lett. A 372 (2008) 670.